The influence of a membrane environment on the structure and stability of a prokaryotic potassium channel, KcsA ☆

J.A. Encinar, M.L. Molina, J.A. Poveda, F.N. Barrera, M.L. Renart,
A.M. Fernández, J.M. González-Ros*

Instituto de Biología Molecular y Celular, Universidad Miguel Hernández, Elche, 03202 Alicante, Spain

Abstract The lack of a membrane environment in membrane protein crystals is considered one of the major limiting factors to fully imply X-ray structural data to explain functional properties of ion channels [Gulbis, J.M. and Doyle, D. (2004) Curr. Opin. Struct. Biol. 14, 440–446]. Here, we provide infrared spectroscopic evidence that the structure and stability of the potassium channel KcsA and its chymotryptic derivative 1–125 KcsA reconstituted into native-like membranes differ from those exhibited by these proteins in detergent solution, the latter taken as an approximation of the mixed detergent-protein crystal conditions.
© 2005 Federation of European Biochemical Societies. Published by Elsevier B.V. All rights reserved.

1. Introduction

The use of high resolution electrophysiological techniques to study ion channels has provided a wealth of information on functional aspects of these important membrane proteins. It has only been recently that such functional information is accompanied by structural knowledge, as several prokaryotic homologues of mammalian ion channels have been purified, crystallized and their structure solved at high resolution (reviewed in [1,2]). Potassium channels have benefited the most from those studies, as the majority of the structures solved belong to this superfamily of ion channels [3–6].

An important application of that knowledge is to use the solved structures to explain fundamental functional properties of these prokaryotic ion channels (such as their gating, ion permeation or selectivity), as well as those exhibited by their phys-

iologically more relevant but structurally ill-defined mammalian homologues. This, however, is not exempt of limitations for several reasons. First, essentially static information (the crystallographic data) is used to explain processes of a dynamic nature (for instance, conformational transitions between closed and open channel states). Second, because highly mobile protein segments are present in these channels, specific antibodies or Fab fragments are frequently used to immobilize them and favor crystallization and structural resolution. This, as MacKinnon himself recognizes [5], might alter the channel structure to a point in which the X-ray data could depart from being an accurate representation of the native conformation. Lastly, the solved structures came from mixed detergent-protein crystals in which the channels are devoid of their native membrane environment, which likely modulates both their structure and function [7,8]. These issues have been recently reviewed [9] and are probably behind the reasons for discrepancies, such as that on the mode of action of the voltage sensor in voltage-dependent potassium channels, which is extensively publicized [10–12].

Here, we report on low resolution, spectroscopic studies on the structural differences exhibited by KcsA, the first potassium channel whose high resolution structure was solved [3], in detergent solution and reconstituted into membranes. We chose such experimental systems because the detergent solution of the purified protein might be the closest experimental system in solution mimicking the mixed detergent-protein crystals used in the X-ray studies. Likewise, reconstitution into a lipid bilayer imitates the channel's native, membrane-bound form. Our results illustrate how just one of the variables commented above, the presence of a native-like membrane environment, determines that the structure adopted by the channel protein departs significantly from those observed in the crystal-mimicking conditions (detergent solution).

2. Materials and methods

2.1. Protein expression and purification

Expression of the wild-type KcsA protein with an added N-terminal hexahistine tag in *Escherichia coli* M15 (pRep4) cells and its purification by affinity chromatography on a Ni^{2+}-NTA agarose column was carried out as reported [13]. The final buffer used with the purified protein was 20 mM HEPES, pH 7.0, containing 100 mM KCl and 1 mM dodecyl β-D-maltoside (DDM).

1–125 KcsA was prepared by chymotrypsin hydrolysis of wild-type KcsA and characterized by MALDI tryptic-peptide mass fingerprinting [13].

2.2. Reconstitution of proteins into asolectin lipid vesicles

Large unilamellar vesicles of asolectin (soybean lipids, type II-S, Sigma) were prepared at 25 mg/ml in 10 mM HEPES, pH 7.0, 100 mM KCl (reconstitution buffer) and stored in liquid N_2 [14] . Purified DDM-solubilized protein was mixed with the above asolectin vesicles previously resolubilized in 3 mM DDM, at a lipid:protein subunit molar ratio of 2000:1, for 2 h. Reconstituted liposomes were formed by removing the detergent by gel filtration on Sephadex G-50 (fine, 15–20 ml bed volume), previously swollen overnight in buffer without detergent. The detergent-solubilized lipid/protein mixture (2 ml) was loaded on top of the column, and the reconstituted liposomes were eluted in the void volume. The protein-containing reconstituted fractions were pooled and centrifuged for 30 min at $300\,000 \times g$. The pellet was suspended into 1 ml of reconstitution buffer, divided into 100 μg aliquots and stored in liquid N_2 [13].

2.3. Fourier transform-infrared spectroscopy

For infrared amide I′ band recordings from detergent-solubilized KcsA samples, aliquots of KcsA in 10 mM HEPES, pH 7.0, containing 100 mM KCl and 1 mM DDM were washed twice with 2 ml of 1 mM HEPES, pH 7.0, 10 mM KCl, 1 mM DDM and its volume reduced to about 200 μl by filtration on Vivaspin concentrators (5000 MW cut off; Vivascience). The concentrated samples were dehydrated in a speed-vac Savant rotary evaporator and resuspended in 20 μl of D_2O to avoid the interference of H_2O infrared absorbance (1645 cm^{-1}). The samples of KcsA reconstituted into asolectin vesicles were submitted to al least two centrifugation–resuspension cycles in D_2O buffers of identical saline composition as those in H_2O.

The resulting samples from either detergent-solubilized or reconstituted KcsA were placed into a liquid demountable cell equipped with CaF_2 windows and 50-μm thick Mylar spacers and maintained at room temperature for approximately 3 h to reach equilibrium [15]. The final amount of protein in the spectrometer cell was approximately 400 μg for each sample.

Infrared spectra were taken in triplicate (600 spectral scans) in a Bruker IF66s instrument equipped with a DTGS detector. Buffer contribution was subtracted from the individual spectra and spectral noise was reduced as described previously [16]. The protein secondary structure was estimated from the IR spectra by decomposition of the amide I′ band into its spectral components [17].

For temperature-dependent studies, the samples were submitted to heating cycles at each at the indicated temperatures. Each step in such heating cycles include (i) a step-like increase in temperature, (ii) an stabilization period of the sample (or plain buffer) in the IR cell at each temperature and (iii) a period of spectral acquisition. The duration of a complete heating cycle was of approximately 2.5 h.

3. Results and discussion

KcsA from *Streptomyces lividans* is a relatively simple member of the potassium channel superfamily [18]. The ease of heterologous expression of KcsA in *E. coli*, its resistance to harsh experimental conditions and its purification in large quantities allowed for its crystallization and structure determination using X-ray diffraction methods [3]. KcsA is a homotetramer in which each subunit is made up of 160 amino acids defining two transmembrane α-helical segments (Fig. 1) connected by a pore region that contains an additional short α-helix and an ion selectivity filter homologous to the more complex eukaryotic potassium channels. The transmembrane segment M2, nearest to the C-terminal, contributes to line the pore, while the one closest to the N-terminal, M1, is exposed to the membrane bilayer [3]. Additionally, the N- and C-termini are included in two cytoplasmic domains, rich in charged or polar amino acids. These domains were not solved in the crystal structure, which accounted only for the membrane-inserted 23–119 amino acids in the KcsA sequence. Nevertheless, electron spin resonance studies predicted that such domains con-
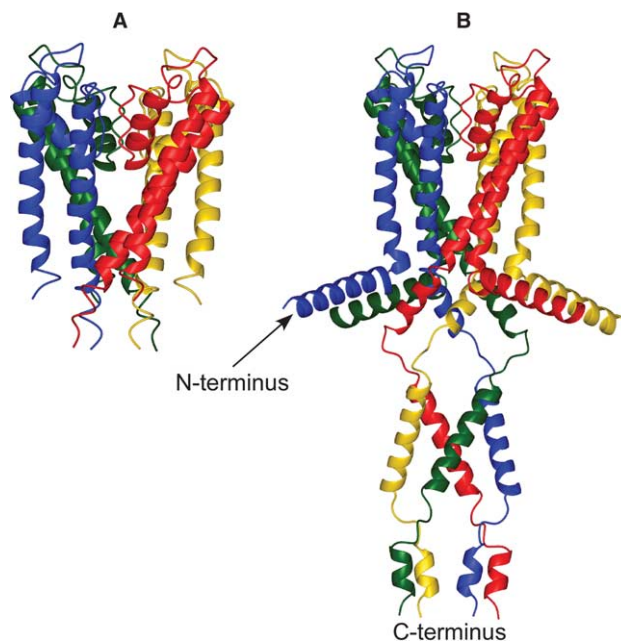

Fig. 1. Structural models for KcsA. (A) represents the 23–119 transmembrane segment of the tetrameric KcsA based on the original X-ray structure (PDB 1BL8) reported by MacKinnon's group from 1 to 125 KcsA crystals [3]. (B) shows a model for the full-length protein derived from using the α-carbon trace of KcsA (PDB 1F6G) reported by Perozo's group [19] as a template, followed by optimization of the resulting structure, as reported earlier [13]. The N- and C-termini have been indicated in the subunit drawn in blue.

tribute additional α-helical motifs to the protein and form a fenestrated "hanging basket"-like structure underneath the membrane [19] (Fig. 1).

Fig. 2 shows infrared amide I′ bands of both, detergent-solubilized and membrane reconstituted KcsA samples. The amide I band (called amide I′ when taken in a D_2O media) comprises the 1600–1700 cm^{-1} spectral region and results primarily from stretching vibrations of C=O groups in peptide bonds [20]. The exact frequencies of such vibrations depend on the nature of the hydrogen bonding involving the C=O groups, which in turn, is determined by the particular secondary structure adopted by the protein [21]. Thus, the amide I band contour represents the composition of overlapping spectral components of characteristic frequencies, which are assigned in H_2O and in D_2O to different secondary structural motifs in both soluble and membrane-bound proteins [22]. In agreement with the abundance of α-helix in the protein's crystal structure, the amide I′ band of the wild-type, 1–160 KcsA in detergent solution (Fig. 2A) is clearly centred at 1655 cm^{-1}, indicating that helical structures are indeed predominant under those conditions. Upon reconstitution into the asolectin lipids (Fig. 2B), however, a shoulder at 1630 cm^{-1} becomes more prominent, indicating that the protein in the membrane-bound form increases its β-sheet contents. Quantitative estimates on the protein's secondary structure were obtained by decomposition of the amide I′ band into its spectral components [17] and confirm that indeed, the changes in spectral shape between detergent-solubilized and membrane-reconstituted samples are primarily due to an increase in the latter of the β-sheet spectral component at 1631 cm^{-1} (Fig. 2C). Previous reports using the full-length protein in transmission and attenuated total reflectance Fourier
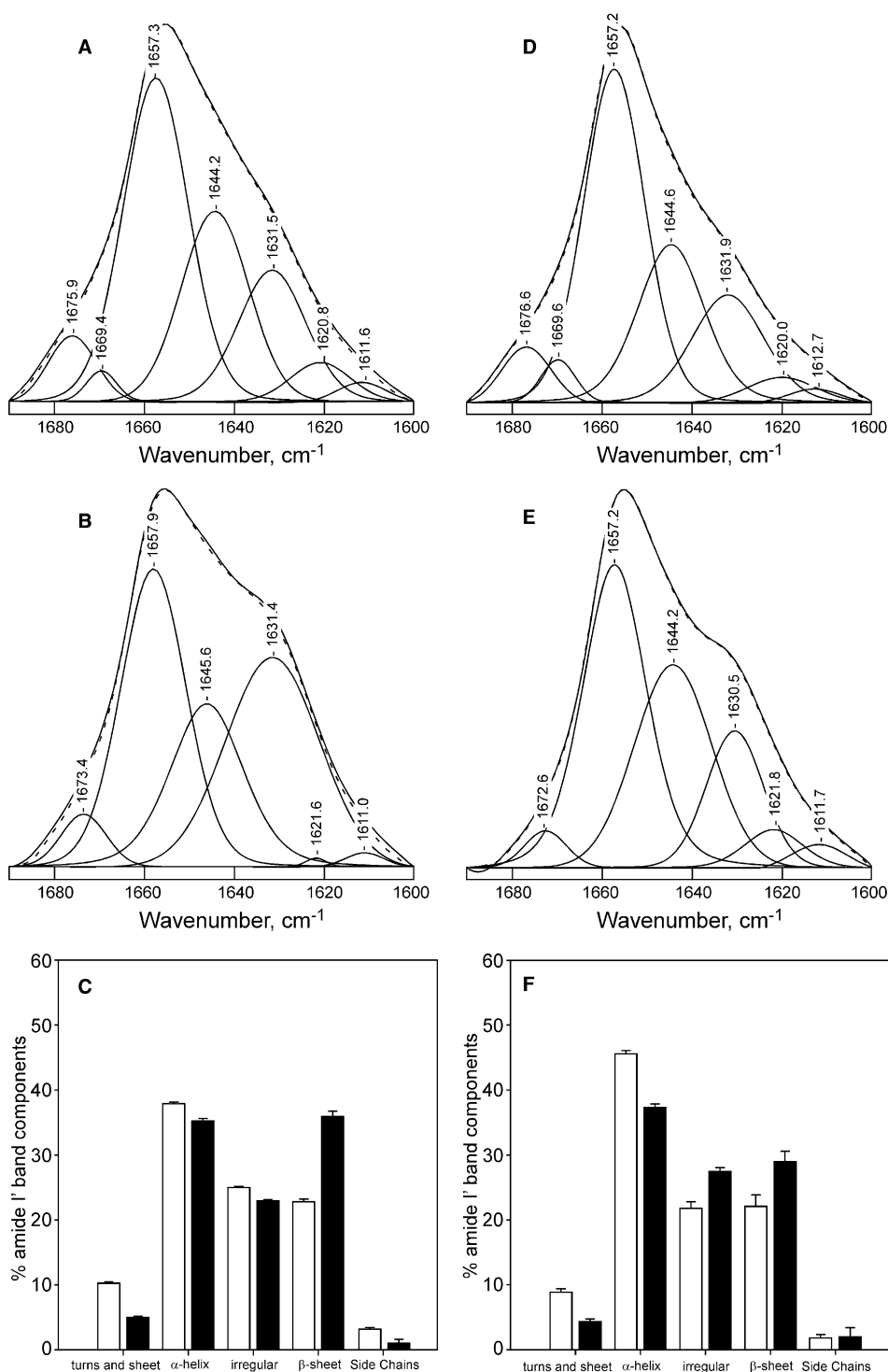
Fig. 2. Representative amide I′ band profiles in the infrared spectra of DDM-solubilized (A) and asolectin-reconstituted (B) wild-type KcsA, and DDM-solubilized (D) and asolectin-reconstituted (E) 1–125 KcsA. All panels include (i) the recorded amide I′ band spectral envelope (continuous line), (ii) the component bands obtained by decomposition of the amide I′ band [17] and (iii) the reconstruction of the amide I′ band from the observed spectral components (dashed line). Band assignments are: 1657 cm^{-1} to α-helix; 1665 and 1690 cm^{-1} to β-turns; 1631 and 1625 cm^{-1} to intramolecular and intermolecular vibrations of β-sheets, respectively; 1644 cm^{-1} to non-ordered conformations, including open loops [31]. Panels C and F show, respectively, the estimated secondary structural elements (in percentages) for the wild-type (C) and 1–125 KcsA (F) in the detergent-solubilized (open bars) and membrane-reconstituted (closed bars) forms. Results in the latter panels are given as means ± S.E., *n* = 3.

transform-infrared spectroscopy (FT-IR) experiments yield comparable secondary structure estimates, but did not show any significant differences between detergent-solubilized and membrane reconstituted samples [15,23].

Fig. 2D, E and F show experiments similar to the above, but obtained with the 1–125 KcsA chymotryptic derivative, the actual protein from which the X-ray crystals were made [3]. The α-helical spectral component at 1657 cm^{-1} in the detergent-

solubilized 1–125 KcsA (Fig. 2D) is even more conspicuous than in the wild-type protein, suggesting that the α-helical contents in the transmembrane region of the protein is higher than that in the whole 1–160 protein sequence. Again, a shoulder at approximately 1630 cm^{-1} is detected upon membrane reconstitution of the 1–125 KcsA protein (Fig. 2E) although now spectral shape differences between the detergent-solubilized and membrane-bound forms are not as large as they were in the wild-type protein. This indicates that the overall structural rearrangement seen in the wild-type protein upon reconstitution includes events within the 1–125 sequence which contain the predominantly transmembrane region and the N-terminal cytoplasmic domain. Estimates of the secondary structure in the detergent-solubilized and reconstituted 1–125 KcsA suggest that the observed spectral shape differences came now mainly from comparable alteration of both, β-structure (1630 cm^{-1}) and non-ordered (1644 cm^{-1}) spectral components (Fig. 2F).

The amide II band in a protein's infrared spectrum (centred at 1547 cm^{-1}) results primarily from NH bending vibrations in the peptide backbone [22,24]. Its residual intensity remaining after extensive D$_2$O exchange arises from non-exchangeable NH groups and therefore, it reports on the inaccessibility of the protein core to the solvent due to tertiary structure. In this respect we found that the residual amide II band (normalized to the amide I′ band intensity to correct for possible differences in protein concentration) from the 1–125 KcsA samples were always more intense that those from wild-type 1–160 KcsA, suggesting that the more α-helical 1–125 protein, having a higher relative contents of transmembrane components, is less accessible to the deuterium exchange than its wild-type counterpart (not shown). Additionally, the rate and extent at which the residual amide II band disappears during thermal denaturation of a protein (as the non-accessible NH protons in the native protein become now exposed) (Fig. 3A) have been taken as an indication of the temperature-induced loss of tertiary contacts [25], which usually occurs at temperatures well below that corresponding to the loss of the protein secondary structure. Fig. 3B illustrates the loss of the residual amide II band as

the temperature is increased in experiments using detergent-solubilized and membrane-bound forms of both, wild-type and 1–125 KcsA. It is observed that the 1–125 KcsA exchanges deuterium as efficiently in the detergent-solubilized and reconstituted forms, suggesting that the protein's tertiary structure is similarly compact in the two environments provided. This seems not to be the case, however, for the wild-type KcsA protein which exchanges somewhat more efficiently in the membrane-bound than in the detergent-solubilized form, thus, suggesting that the 126–160 protein segment becomes more accessible to the solvent upon reconstitution into membranes. Such an enhanced solvent accessibility and loss of tertiary contacts occur with no apparent cooperativity and at temperatures lower than those corresponding to the loss of secondary structure, as monitored by the temperature dependence of the amide I′ band described below.

The thermal dependence of the amide I′ band (Fig. 4A) has been used to assess the stability of the protein secondary structure. Thermal denaturation results in amide I′ band widening and other spectral changes, including the appearance of components at 1620 and 1684 cm^{-1}, which are related to aggregation of thermally denatured proteins [26]. KcsA is remarkably stable in all cases and temperatures above 100 °C are needed for thermal denaturation. Fig. 4B shows that the secondary structure of the 1–125 KcsA protein is similarly stable in the detergent-solubilized or membrane-reconstituted forms. In either condition, this protein exhibits a midpoint temperature for the thermal denaturation process around 109 °C. On the other hand, the wild-type KcsA in the detergent-solubilized form is more stable than the 1–125 KcsA in either of the two conditions from above, and shows a midpoint temperature for the denaturation process at approximately 113 °C. Such increased stability, which seems partly attributable to the 126–160 protein segment present in the wild-type KcsA, is even further increased upon reconstitution, in which the midpoint denaturation temperature reaches values as high as 117 °C. This suggests that it is not only the presence of the 126–160 segment, but also the different environment provided by the reconstituted membrane, what confers increased
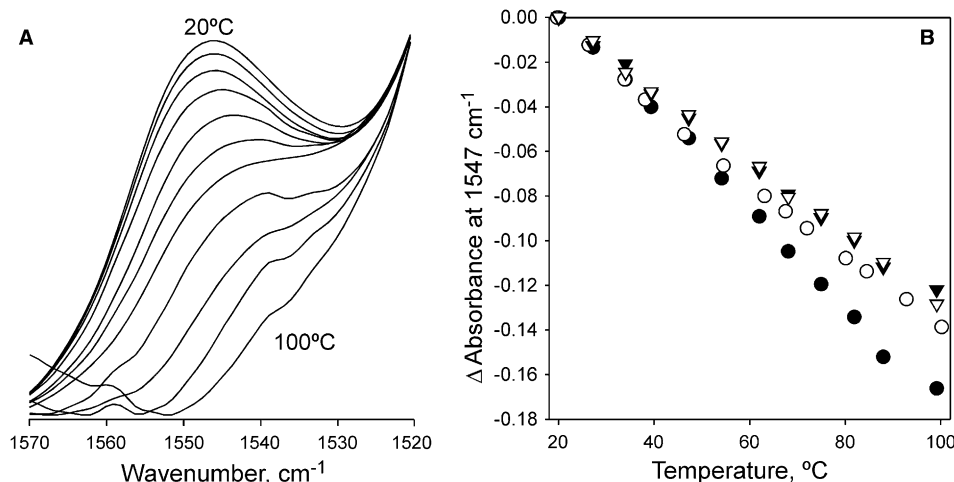

Fig. 3. Analysis of the residual amide II infrared band of KcsA. (A) illustrates the temperature-dependent changes in the 1570–1520 cm^{-1} infrared region in a reconstituted, wild-type KcsA sample. (B) shows the loss of the 1547 cm^{-1} absorbance maximum with temperature for DDM-solubilized (○) and asolectin reconstituted (●) wild-type KcsA samples, as well as those corresponding to DDM-solubilized (▽) and asolectin reconstituted (▼) 1–125 KcsA. Data are expressed as the differential absorbance value resulting from subtracting the amide II band taken at 20 °C in each of the samples from those obtained as the temperature is increased. Three different series of samples were used in these studies yielding essentially identical results.
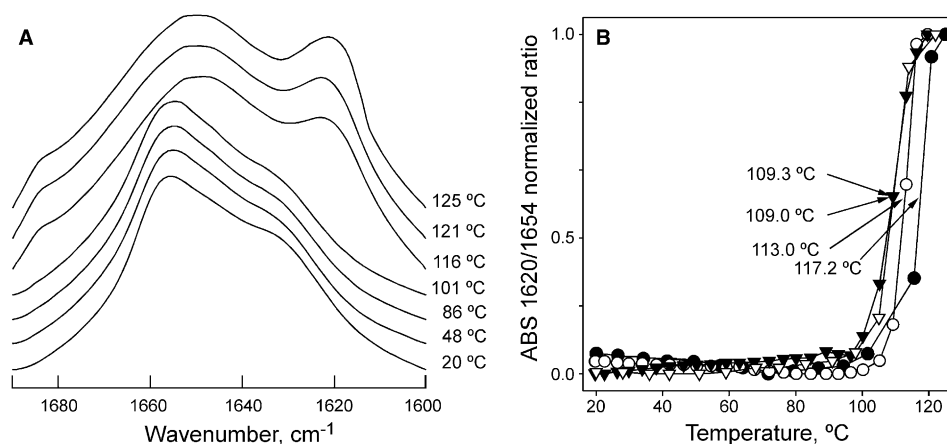
Fig. 4. Temperature dependence of the amide I′ band of KcsA. (A) illustrates the temperature-dependent changes in a wild-type KcsA reconstituted sample taken as an example. Temperatures of spectral acquisition are indicated. (B) shows the temperature dependence of the spectral changes seen in all samples in terms of the normalized 1620–1654 cm^{-1} absorbance ratio. Numbers within the panel indicate the estimated midpoint temperatures for thermal denaturation of the proteins in the different experimental conditions. Symbols are: DDM-solubilized (○) and reconstituted wild-type KcsA (●); DDM-solubilized (▽) and reconstituted 1–125 KcsA (▼). Error bars from three different experiments are smaller than the size of the symbols used in the drawing.

thermal stability to the wild-type protein secondary structure. Previous SDS–PAGE studies on thermally induced dissociation into subunits of the tetrameric KcsA [13,27,28] did not clearly established a stabilizing role for the 126–160 protein segment, but definitively identified the lipids also as stabilizers of the tetrameric assembly in both, wild type and 1–125 KcsA [13].

In summary, we have used the wild-type and the 1–125 chymotryptic derivative of KcsA to illustrate how important features of these proteins such as their secondary structure, accessibility to the solvent and thermal stability become altered under experimental conditions trying to imitate crystal-like or native-like environments. The reasons for structural alteration in the different experimental conditions (protein crystals, detergent solutions, reconstituted membranes and so on) are likely to be found both, in specific interactions with specific components present in some of the experimental systems under study (protein-lipid interactions in membranes or antibody interactions in the mixed detergent-protein crystals), as well as in the different packing constrains imposed or in the need for shielding exposed hydrophobic residues. These latter aspects might be particularly important in this case as it is known that the hydrophobic thickness of the transmembrane portion of KcsA is about 37 Å, while that of a typical biological membrane is about 27 Å [29]. In spite of such differences, KcsA is known to maintain an efficient hydrophobic matching when reconstituted into bilayers with very different chain lengths [30] and thus, it is expected that the tilt angle of the transmembrane helices of KcsA, which is about 25° with respect to the normal to the membrane in the crystal structure, increases much further when membrane-bound to accommodate to the bilayer thickness. Such an increased tilting and the resulting stretch imposed on the protein might partly be responsible for the differences observed here in protein structure and stability. Circumstances such as the above might also be applicable to other membrane proteins besides KcsA and therefore, caution must be exercised when trying to rigorously extrapolate X-ray high resolution structural data to explain experimental results obtained under physiological-like conditions.

References

[1] Booth, I.R., Edwards, M.D. and Miller, S. (2003) Bacterial ion channels. Biochemistry 42, 10045–10053.

[2] MacKinnon, R. (2003) Potassium channels. FEBS Lett. 555, 62–65.

[3] Doyle, D.A., Morais, C.J., Pfuetzner, R.A., Kuo, A., Gulbis, J.M., Cohen, S.L., Chait, B.T. and MacKinnon, R. (1998) The structure of the potassium channel: molecular basis of K$^+$ conduction and selectivity. Science 280, 69–77.

[4] Jiang, Y., Lee, A., Chen, J., Cadene, M., Chait, B.T. and MacKinnon, R. (2002) Crystal structure and mechanism of a calcium-gated potassium channel. Nature 417, 515–522.

[5] Jiang, Y., Lee, A., Chen, J., Ruta, V., Cadene, M., Chait, B.T. and MacKinnon, R. (2003) X-ray structure of a voltage-dependent K$^+$ channel. Nature 423, 33–41.

[6] Kuo, A., Gulbis, J.M., Antcliff, J.F., Rahman, T., Lowe, E.D., Zimmer, J., Cuthbertson, J., Ashcroft, F.M., Ezaki, T. and Doyle, D.A. (2003) Crystal structure of the potassium channel KirBac1.1 in the closed state. Science 300, 1922–1926.

[7] Lee, A.G. (2004) How lipids affect the activities of integral membrane proteins. Biochim. Biophys. Acta 1666, 62–87.

[8] Valiyaveetil, F.I., Zhou, Y. and MacKinnon, R. (2002) Lipids in the structure, folding, and function of the KcsA K$^+$ channel. Biochemistry 41, 10771–10777.

[9] Gulbis, J.M. and Doyle, D.A. (2004) Potassium channel structures: do they conform? Curr. Opin. Struct. Biol. 14, 440–446.

[10] Ahern, C.A. and Horn, R. (2004) Stirring up controversy with a voltage sensor paddle. Trends Neurosci. 27, 303–307.

[11] Starace, D.M. and Bezanilla, F. (2004) A proton pore in a potassium channel voltage sensor reveals a focused electric field. Nature 427, 548–553.

[12] Gonzalez, C., Morera, F.J., Rosenmann, E., Alvarez, O. and Latorre, R. (2005) S3b amino acid residues do not shuttle across the bilayer in voltage-dependent Shaker K$^+$ channels. Proc. Natl. Acad. Sci. USA 102, 5020–5025.

[13] Molina, M.L., Encinar, J.A., Barrera, F.N., Fernandez-Ballester, G., Riquelme, G. and Gonzalez-Ros, J.M. (2004) Influence of C-terminal protein domains and protein–lipid interactions on

tetramerization and stability of the potassium channel KcsA. Biochemistry 43, 14924–14931.

[14] Riquelme, G., Lopez, E., Garcia-Segura, L.M., Ferragut, J.A. and Gonzalez-Ros, J.M. (1990) Giant liposomes: a model system in which to obtain patch-clamp recordings of ionic channels. Biochemistry 29, 11215–11222.

[15] le Coutre, J., Kaback, H.R., Patel, C.K., Heginbotham, L. and Miller, C. (1998) Fourier transform infrared spectroscopy reveals a rigid alpha-helical assembly for the tetrameric *Streptomyces lividans* K$^+$ channel. Proc. Natl. Acad. Sci. USA 95, 6114–6117.

[16] Echabe, I., Encinar, J.A. and Arrondo, J.L.R. (1997) Removal of spectral noise in the quantitation of protein structure through infrared band decomposition. Biospectroscopy 3, 469–475.

[17] Encinar, J.A., Mallo, G.V., Mizyrycki, C., Giono, L., Gonzalez-Ros, J.M., Rico, M., Canepa, E., Moreno, S., Neira, J.L. and Iovanna, J.L. (2001) Human p8 is a HMG-I/Y-like protein with DNA binding activity enhanced by phosphorylation. J. Biol. Chem. 276, 2742–2751.

[18] Schrempf, H., Schmidt, O., Kummerlen, R., Hinnah, S., Muller, D., Betzler, M., Steinkamp, T. and Wagner, R. (1995) A prokaryotic potassium ion channel with two predicted transmembrane segments from *Streptomyces lividans*. EMBO J. 14, 5170–5178.

[19] Cortes, D.M., Cuello, L.G. and Perozo, E. (2001) Molecular architecture of full-length KcsA: role of cytoplasmic domains in ion permeation and activation gating. J. Gen. Physiol. 117, 165–180.

[20] Susi, H. (1972) Infrared spectroscopy – conformation. Methods Enzymol. 26 PtC, 455–472.

[21] Susi, H., Timasheff, S.N. and Stevens, L. (1967) Infrared spectra and protein conformations in aqueous solutions. I. The amide I band in H$_2$O and D$_2$O solutions. J. Biol. Chem. 242, 5460–5466.

[22] Surewicz, W.K. and Mantsch, H.H. (1988) New insight into protein secondary structure from resolution-enhanced infrared spectra. Biochim. Biophys. Acta 952, 115–130.

[23] Tatulian, S.A., Cortes, D.M. and Perozo, E. (1998) Structural dynamics of the *Streptomyces lividans* K$^+$ channel (SKC1): secondary structure characterization from FTIR spectroscopy. FEBS Lett. 423, 205–212.

[24] Dousseau, F. and Pezolet, M. (1990) Determination of the secondary structure content of proteins in aqueous solutions from their amide I and amide II infrared bands. Comparison between classical and partial least-squares methods. Biochemistry 29, 8771–8779.

[25] van Stokkum, I.H., Linsdell, H., Hadden, J.M., Haris, P.I., Chapman, D. and Bloemendal, M. (1995) Temperature-induced changes in protein structures studied by Fourier transform infrared spectroscopy and global analysis. Biochemistry 34, 10508–10518.

[26] Surewicz, W.K., Leddy, J.J. and Mantsch, H.H. (1990) Structure, stability, and receptor interaction of cholera toxin as studied by Fourier-transform infrared spectroscopy. Biochemistry 29, 8106–8111.

[27] Perozo, E., Cortes, D.M. and Cuello, L.G. (1999) Structural rearrangements underlying K$^+$-channel activation gating. Science 285, 73–78.

[28] van Dalen, A., Hegger, S., Killian, J.A. and de Kruijff, B. (2002) Influence of lipids on membrane assembly and stability of the potassium channel KcsA. FEBS Lett. 525, 33–38.

[29] Williamson, I.M., Alvis, S.J., East, J.M. and Lee, A.G. (2003) The potassium channel KcsA and its interaction with the lipid bilayer. Cell Mol. Life Sci. 60, 1581–1590.

[30] Williamson, I.M., Alvis, S.J., East, J.M. and Lee, A.G. (2002) Interactions of phospholipids with the potassium channel KcsA. Biophys. J. 83, 2026–2038.

[31] Arrondo, J.L., Castresana, J., Valpuesta, J.M. and Goni, F.M. (1994) Structure and thermal denaturation of crystalline and noncrystalline cytochrome oxidase as studied by infrared spectroscopy. Biochemistry 33, 11650–11655.